This journal is (c) The Royal Society of Chemistry 2010

Supporting information for the manuscript

New insights into the acid mediated disproportionation of pentavalent uranyl

*Victor Mougel, Biplab Biswas, Jacques Pécaut and Marinella Mazzanti**

Contribution from

Laboratoire de Reconnaissance Ionique et Chimie de Coordination, Service de Chimie Inorganique et Biologique (UMR-E 3 CEA-UJF, FRE 3200 CNRS), INAC, CEA-Grenoble, 38054 GRENOBLE, Cedex 09, France.

Fax: (+)33(0)438785090 ; E-mail: marinella.mazzanti@cea.fr

*Correspondence to Dr. Marinella Mazzanti

General considerations.

All manipulations were carried out under an inert argon atmosphere using Schlenk techniques and an MBraun glovebox equipped with a purifier unit. The water and oxygen level were always kept at less than 1 ppm. The solvents were purchased from Aldrich in their anhydrous form conditioned under argon and were vacuum distilled from K/benzophenone (diisopropylether, hexane, pyridine and THF) or CaH_2 (acetonitrile). Depleted uranium turnings were purchased from the "Société Industrielle du Combustible Nucléaire" of Annecy (France). Benzoic acid and potassium benzoate were purchased from Aldrich. Benzoic acid was purified by sublimation and potassium benzoate was dried under high *vacuum* for one week at 40°C. $[UI_3(thf)_4]$[1], $[UI_4(CNPh)_4]$[2] and $[(UO_2Py_5)(KI_2Py_2)]$[3] were synthesized as previously described.

UV-Visible measurements were carried out with a Varian Cary 50 Probe spectrophotometer in quartz cells (optical path lengths: 1 mm) adapted with Young valves.

Elemental analyses were performed under argon by Analytische Laboratorien GMBH at Lindlar, Germany.

^{1}H NMR spectra were recorded on Bruker 200 MHz and 500 MHz spectrometers. NMR chemical shifts are reported in ppm with solvent as internal reference.

Synthesis

Synthesis of $[U_6O_4(OH)_4(C_6H_5COO)_{12}(Py)_x]$. 2MeCN:

From uranyl(V): see footnotes

From U(III):

An acetonitrile (0.5 mL) solution of potassium benzoate (7.1 mg, 0.044 mmol) was reacted with an acetonitrile solution (0.5 ml) of $UI_3(THF)_4$ (20.0 mg, 0.022 mmol). 88 μL of a 0.5 M solution of water (0.044 mmol) in acetonitrile was added to the resulting green colour solution. The resulting dark green solution was stirred over 1 day at room temperature, filtered and then evaporated to dryness under vacuum. The resulting green solid was dissolved in pyridine (1 mL) and diisopropyl ether (1 mL) was added, causing the formation of white precipitate of KI which was removed after 2 days by filtration. The resulting green solution was evaporated to dryness and the residue was recrystallized in acetonitrile, X-ray quality crystals of **1.2MeCN** were obtained over 6-7 hours in 75 % yield.

From U(IV):

Crystals of **1** were also obtained starting from $[UI_4(PhCN)_4]$, by reacting a pyridine solution (0.5 mL) of potassium benzoate (5.5 mg, 0.034 mmol) with a solution of $UI_4(PhCN)_4$ (20.0 mg, 0.017 mmol) in pyridine (0.5 ml). 68 μL of a 0.5(M) water solution in pyridine (0.034 mmol) was added to this mixture to yield, after 1 day stirring at room temperature, a green solution with an off-white precipitate. The precipitate was filtered out and the resulting green solution was evaporated under reduced pressure to yield a light green solid, which was recrystallized in acetonitrile. The structure of cluster **1** was confirmed by X-Ray diffraction.

Solution studies:

Figure S1: Proton NMR spectrum (1.7mM) of **1** (Bruker Advance 500MHz).

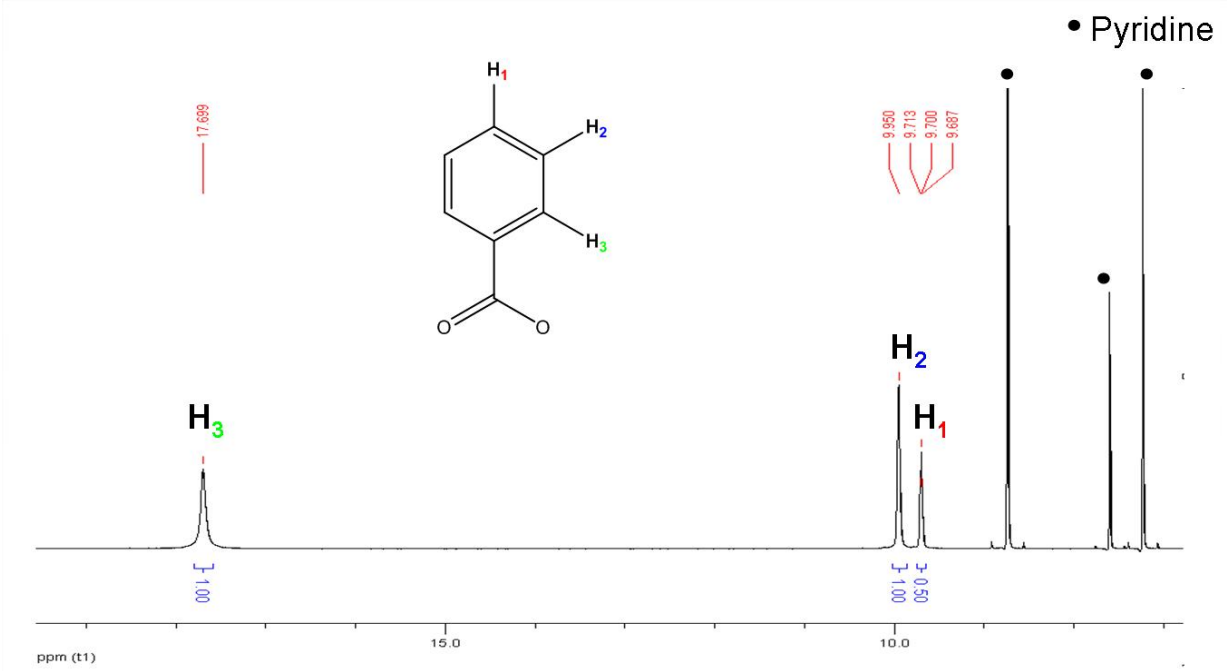

Figure S2: Proton NMR spectrum of **2** (2.5mM) (Bruker 200MHz).

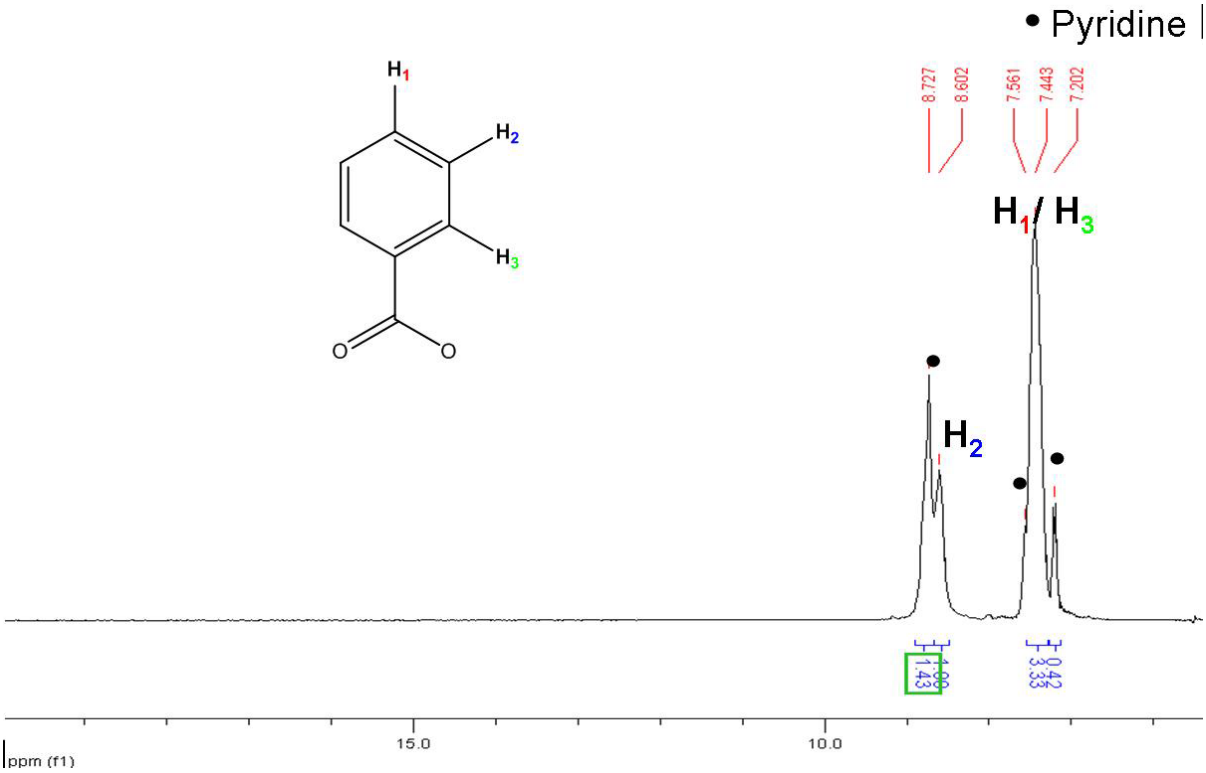

Figure S3: UV-Visible spectra of **1** (blue) and **2** (red) in pyridine solution

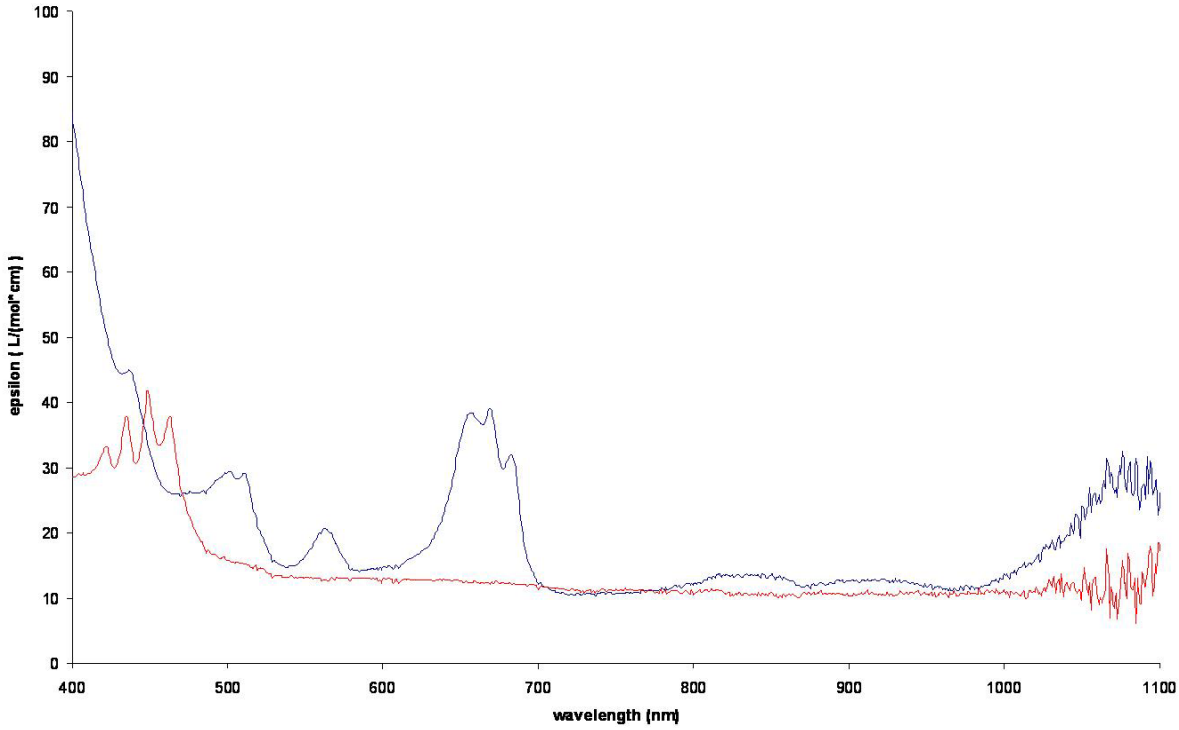

Characterisation of water in the reaction mixture after the disproportionation reaction.

A solution of 6.8 mg of benzoic acid (0.055 mmol, 2 eq) in 0.5 mL of pyridine-d_5 was added to a red suspension of 31 mg of $[(UO_2Py_5)(KI_2Py_2)]$ (0.027 mmol, 1 eq) in 0.5 mL pyridine-d_5, yielding after 10 minutes stirring a clear green solution. The resulting solution was stirred an additional 2h, and was transferred in a NMR tube. The ^{1}H NMR spectra of the mixture presents the peaks of the species **1** and **2**, but also an additional broad peak at 14.51 ppm (Figure S4 -1). The addition of 0.5 equivalent of water to this sample led to the decrease of the shift of this peak to 13.29 ppm together with an increase of its intensity , and no peak were observed at the usual place for water in pyridine (around 5 ppm) (Figure S4 -2). When this solution was taken to dryness and dissolved back in pyridine, the shift of the additional peak increased up to 17.50 ppm with a significant decrease of its intensity (Figure S4 -3). This behaviour is characteristic of the N-H$^+$ proton of pyridinium in pyridine in presence of water, and has been studied in detail.[4] The final peak observed at 17.50 ppm has been observed by Schuppert *et al*.[4] for the pure pyridinium proton, which also noticed that the addition of water

to a pyridinium chloride solution in pyridine led to the decrease of the shift of the pyridinium proton and no peak at the usual shift for water.

Figure S4: Proton NMR spectra of the reaction mixture: 1 - crude mixture; 2 - after addition of 0.5 eq of water; 3 - after drying under vacuum (Bruker 200MHz, *: pyridine residual peaks).

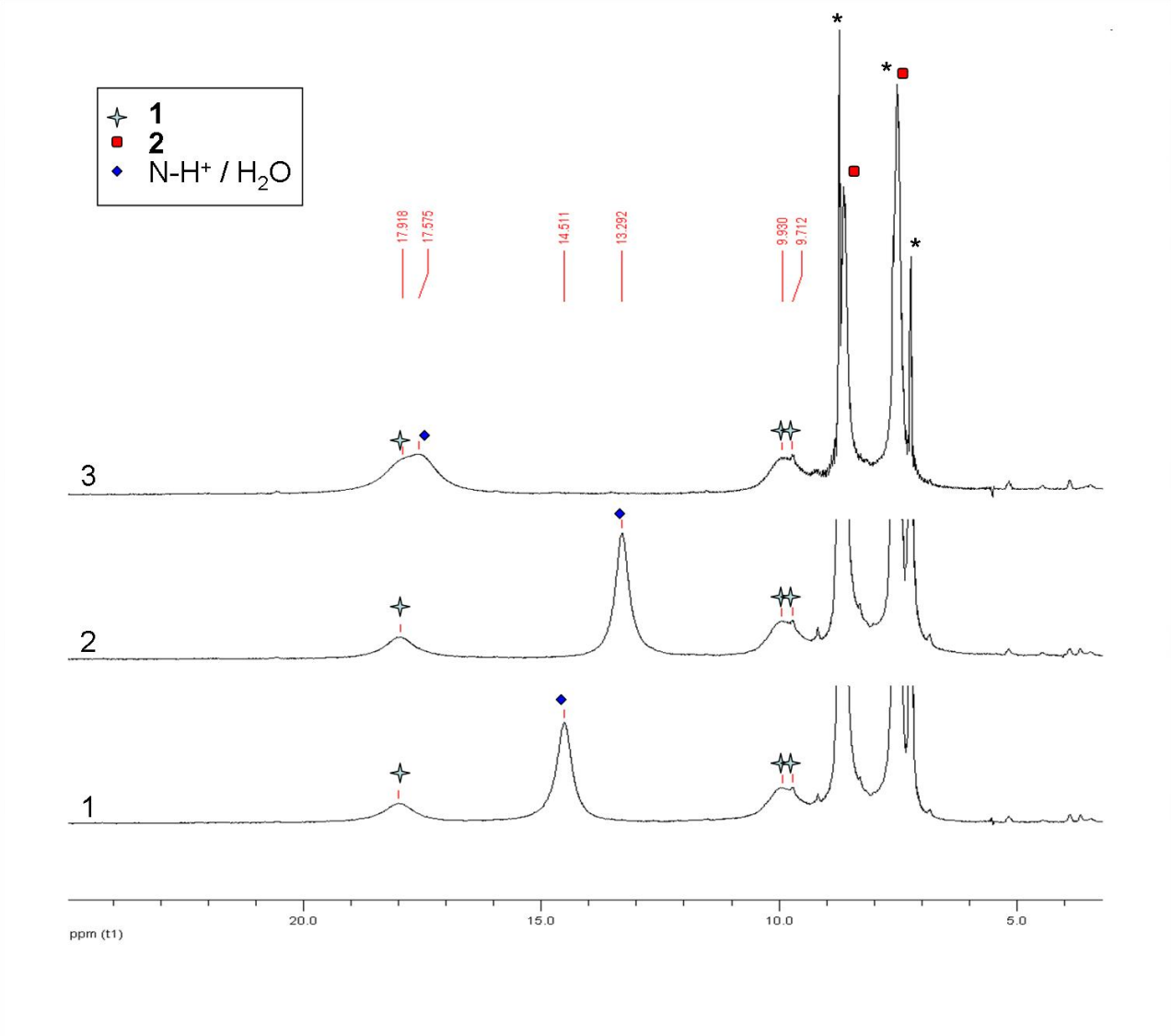

Deconvolution

The ^{1}H NMR of the reaction mixture was fitted using the deconvolution tool provided with the software Mestrec 4.8.6.0 in the windows 22-5 ppm. To minimize systematic errors arising from applying Lorentzian or Gaussian lineshapes, a mixed Lorentzian-Gaussian (Voight) lineshape model was used for the deconvolution. The experimental peaks were first fitted using the Levenberg-Marquardt non–linear least squares and Downhill Simplex (Nelder and Mead) algorithms for estimating peak parameters (position, intensity, line width and lineshape function).

A ratio **1**:**2** of 1:1.25 was finally determined with this refined model.

Table S1: Parameters used to model the different peaks of the reaction mixture NMR with the Mestrec program(L/G: Lorentzian-Gaussian ratio of the Voight function)

Peak	ppm	Height	Width	L/G	Area	Normalised area	assignement
0	17,945	568	166	1	148107,244	1	**H3 cluster**
1	14,488	2886,55	73	1	330995,302	2,23	N-H+/H2O
2	9,91	937	145	1	213416,243	1,44	**H1/H2 cluster**
3	9,692	302	16	1	7590,088	0,05	
4	9,15	571	4	1	3587,699	0,02	pyridine ^{13}C satellite
5	8,716	35911	11,58	0,5	547936,311	3,69	pyridine
6	8,606	8600	14,3	1	193176,535	1,30	**H3 monomer**
7	7,571	9056	20,6	1	293037,715	1,97	pyridine
8	7,473	7099	22,5	1	250899,37	1,69	**H1/H2 monomer**
9	7,211	16018	11,6	1	291867,79	1,97	pyridine

Figure S5: Graphical representation of the peaks represented in Table S1.

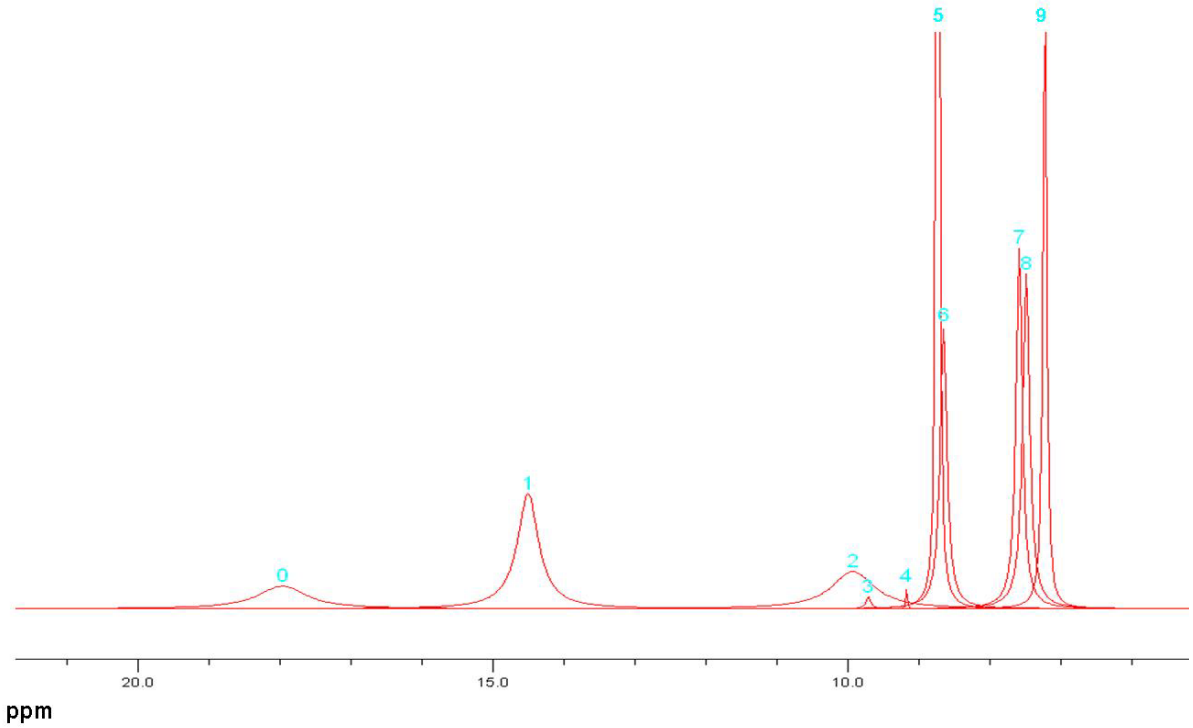

Figure S6: Graphical representation of the peaks in Table S1 (grey line) and original NMR spectra (dark line).

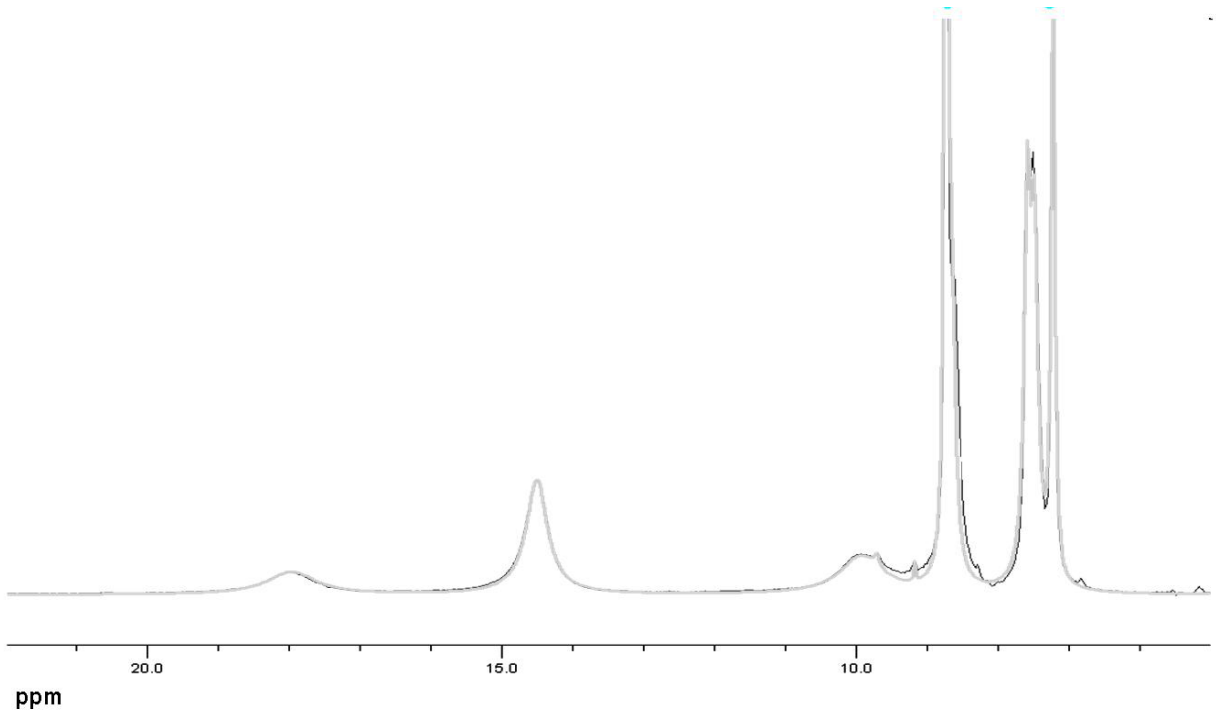

Figure S7: Difference between the calculated and experimental spectrum (brown line), and experimental NMR spectra (dark line)

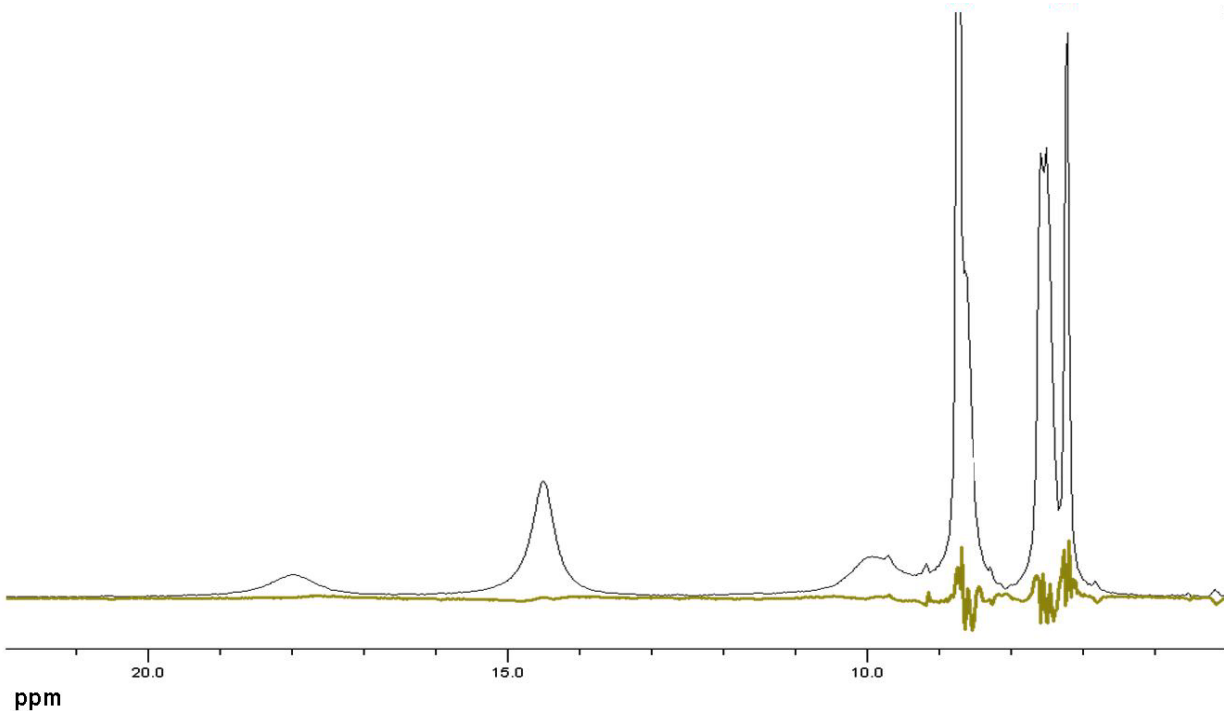

Stability studies in presence of water

4.8 mg of **1** (0.0013 mmol) were dissolved in 1 mL pyridine-d_5 and 200 µL of a 0.5 M solution of water in pyridine (0.40 mmol, 50 eq per U atom) was added to this light green solution. No changes were observed in the ^{1}H NMR spectra before and after the water addition. This solution was followed in time by ^{1}H NMR and no decomposition was observed after two weeks.

X-Ray Crystallography.

Diffraction data were taken using a Oxford-Diffraction XCallibur S kappa geometry diffractometer (Mo-Kα radiation, graphite monochromator, λ = 0.71073 Å). To prevent evaporation of co-crystallized solvent molecules the crystals were coated with light hydrocarbon oil and the data were collected at 150 K. The cell parameters were obtained with intensities detected on three batches of 5 frames. The crystal-detector distance was 4.5 cm. The number of settings and frames has been established taking in consideration the Laue symmetry of the cell by CrysAlisPro Oxford-diffraction software, Version 1.171.33.52. 131 and 247 narrow data were collected for 1° increments in ω with a 60 s and 1.5 s exposure times for **1** and **2.** Unique intensities detected on all frames using the Oxford-diffraction Red program were used to refine the values of the cell parameters. The substantial redundancy in data allows empirical absorption corrections to be applied using multiple measurements of equivalent reflections with the ABSPACK Oxford-diffraction program. Space groups were determined from systematic absences, and they were confirmed by the successful solution of the structure. The structures were solved by direct methods using the SHELXTL 6.14 package and for all structures all atoms, excepted hydrogen atoms, were found by difference Fourier syntheses. All non-hydrogen atoms were anisotropically refined on F^2. Hydrogens were placed in ideal position and refined as riding model.

Figure S8. a) Ortep view of $[U_6O_4(OH)_4(C_6H_5COO)_{12}Py_3]$.2MeCN and b) Mercury view of the central core with thermal ellipsoids at the 30% probability level. Hydrogen atoms of the ligand and aromatic cycles were omitted for clarity. (Uranium are represented in green, oxygen in red carbon in grey and nitrogen in blue.) Selected distances (Å) and angles (deg): U(1)-U(2) 3.858(3), U(2)-U(3) 3.823(3), U(2)-U(2) 3.8327(15), U(1)-O(1U) 2.453(17), U(1)-O(2U) 2.23(2), U(2)-O(2U) 2.271(13), U(2)-O(1U) 2.427(13), U(2)-O(3U) 2.455(15), U(3)-O(3U) 2.42(2), U(3)-O(4U) 2.25(2) and O(2U)-U(1)-O(2U) 90.5(11), O(2U)-U(1)-O(1U) 68.6(4), O(4U)-U(2)-O(2U) 91.4(7), O(4U)-U(2)-O(1U) 68.8(7), O(2U)-U(2)-O(1U) 68.4(6), O(4U)-U(2)-O(3U) 69.7(6), O(4U)-U(3)-O(4U) 92.7(11), O(4U)-U(3)-O(3U) 70.5(4), U(2)-U(2)-U(2) 89.998(1).

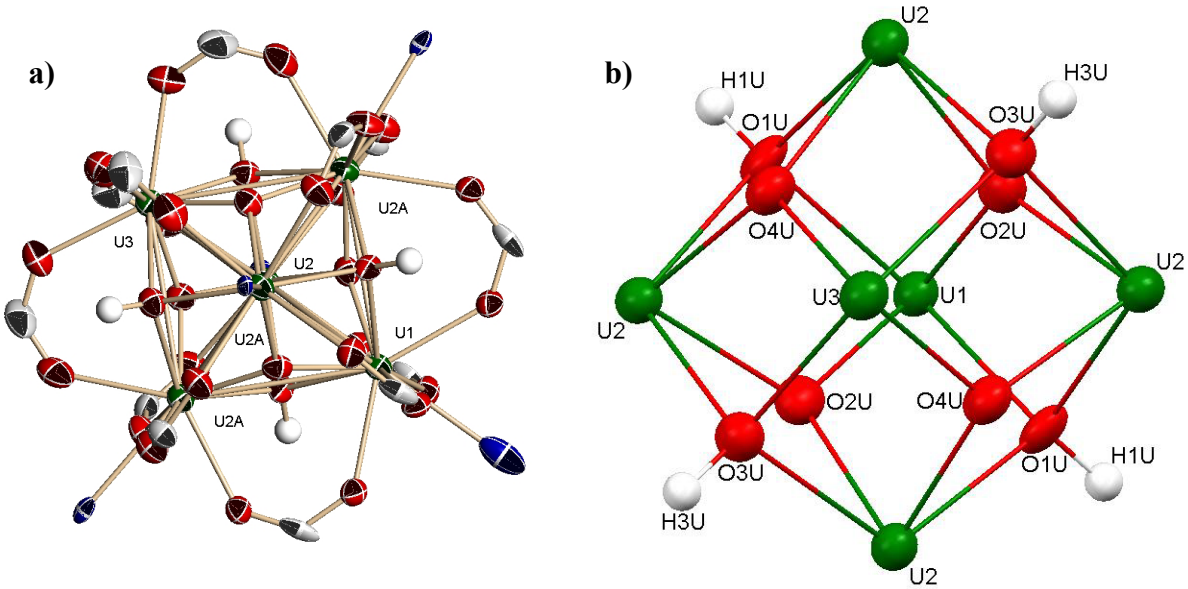

Table S2. Crystallographic data of $[U_6O_4(OH)_4(C_6H_5COO)_{12}Py_3]$.2MeCN

structural parameters	**$[U_6O_4(OH)_4(C_6H_5COO)_{12}(Py)_3]$.2MeCN**
Empirical formula	C103 H85 N5 O32 U6
Formula weight	3332.94
Temperature	150(2) K
Wavelength	0.71073 A
Crystal system	Orthorhombic
Space group	C mcm
Unit cell dimensions	a = 27.493(3) A alpha = 90 deg.
	b = 16.418(18) A beta = 90 deg.
	c = 28.809(3) A gamma = 90 deg.
Volume, Z	13004(15) A^3, 4
Density (calculated)	1.702 Mg/m^3
Absorption coefficient	7.511 mm^{-1}
F(000)	6184
Crystal size	0.15 x 0.10 x 0.04 mm
Theta range for data collection	3.28 to 26.37 deg.
Limiting indices	-34<=h<=17, -20<=k<=9, -35<=l<=34
Reflections collected	16195
Independent reflections	6878 [R(int) = 0.0896]
Absorption correction	Semi-empirical from equivalents
Max. and min. transmission	0.7790 and 0.4027
Refinement method	Full-matrix least-squares on F^2
Data / restraints / parameters	6878 / 102 / 407
Goodness-of-fit on F^2	0.758
Final R indices [I>2sigma(I)]	R1 = 0.0833, wR2 = 0.1985
R indices (all data)	R1 = 0.1822, wR2 = 0.2245
Largest diff. peak and hole	3.634 and -2.019 $e.A^{-3}$

Figure S9. Ortep view of $[UO_2(C_6H_5COO)_2(Py)_2]$ with thermal ellipsoids at the 30% probability level. Hydrogen atoms were omitted for clarity. (Uranium are represented in green, oxygen in red carbon in grey and nitrogen in blue.) Selected distances (Å) and angles (deg): U(1)-O(3) 1.769(5), U(1)-O(2) 2.476(5), U(1)-O(1) 2.478(5), U(1)-N(1) 2.592(6), and O(3)-U(1)-O(3)#1 180.0, O(2)-U(1)-N(1)#1 63.62(17), O(2)#1-U(1)-O(1) 127.87(15).

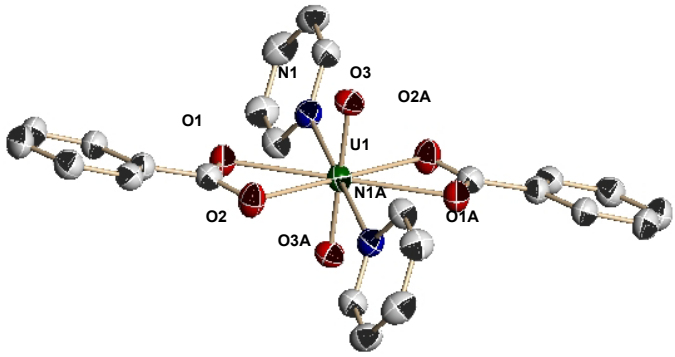

Table S3. Crystallographic data of $[UO_2(C_6H_5COO)_2Py_2]$

structural parameters	**$[UO_2(C_6H_5COO)_2Py_2]$**
Empirical formula	C24 H20 N2 O6 U
Formula weight	670.45
Temperature	150(2) K
Wavelength	0.71073 A
Crystal system	Monoclinic
Space group	P 2_1/c
Unit cell dimensions	a = 11.3216(9) A alpha = 90 deg. b = 10.0554(8) A beta = 95.493(8) deg. c = 10.1130(8) A gamma = 90 deg.
Volume, Z	1146.00(16) A^3, 2
Density (calculated)	1.943 Mg/m^3
Absorption coefficient	7.124 mm^{-1}
F(000)	636
Crystal size	1.06 x 0.57 x 0.39 mm
Theta range for data collection	3.49 to 32.52 deg.
Limiting indices	-16<=h<=17, -11<=k<=14, -14<=l<=5
Reflections collected	6840
Independent reflections	3712 [R(int) = 0.0248]
Absorption correction	Semi-empirical from equivalents
Max. and min. transmission	0.1662 and 0.0494
Refinement method	Full-matrix least-squares on F^2
Data / restraints / parameters	3712 / 0 / 151
Goodness-of-fit on F^2	0.978
Final R indices [I>2sigma(I)]	R1 = 0.0582, wR2 = 0.1428
R indices (all data)	R1 = 0.0815, wR2 = 0.1499
Largest diff. peak and hole	5.148 and -1.111 $e.A^{-3}$

Bond Valence Sum Calculations.

The oxidation state for each uranium atom was calculated using the formula: $V_i = \sum s_{ij}$, (considering the bond valence for the atom i $s_{ij} = \exp[(r_{ij} - d_{ij})/b]$, where d_{ij} is the experimental bond length while r_{ij} and b are empirically determined constants for the given *i-j* bond) proposed by Brown[5] for al U–X bonds in $[U_6O_4(OH)_4(C_6H_5COO)_{12}Py_3]$.2MeCN. We used the parameters published on the Web[6] $r_{ij} = 2.112$ and $b = 0.37$ for U–O bonds and $r_{ij} = 2.18$ and $b = 0.37$ for U–N bonds. The summary of bond valences sum calculation is presented in Table S4.

Table S4. Bond valence sum for $[U_6O_4(OH)_4(C_6H_5COO)_{12}Py_3]$.2 MeCN

Atom	U(1)	U(2)	U(3)
V	3.90	3.97	4.05

The numbers in brackets refer to the indexing of uranium atoms shown on the Ortep view on Figure S8.

Diffusion coefficient measurement

The diffusion NMR experiments were performed using a Pulsed-Field Gradient STimulated Echo (PFGSTE) sequence, using bipolar Gradients, at 298 K and no spinning was applied to the NMR tube.[7-9]

The following BPP-LED (**B**ipolar **P**ulse **P**air – **L**ongitudinal **E**ddy-current **D**elay) pulse sequence was applied:[8]

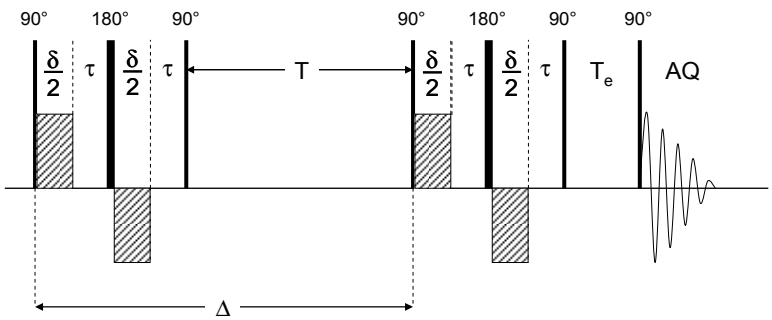

$\delta = 5$ ms. $\tau = 0.4$ ms.

The diffusion times T were optimized for **1** in pyridine at 200 ms. The evolution of the pulsed-field gradient during the NMR diffusion experiments was established in 25 steps, applied linearly between 1 and 30 $G.cm^{-1}$.

In the present sequence the intensity of the signal is given by the following equation: [8]

$$I(q) = I(0).\exp\left[-D.q^2.\left(\Delta - \frac{\delta}{3} - \frac{\tau}{2}\right)\right]$$

were $q = \gamma.\delta.g$

D: diffusion coefficient ($m^2.s^{-1}$)

Δ: time between the two gradient pulse sequences (s)

δ: bipolar gradient duration (s)

τ: pulse separation delay (s)

γ: magnetogyric ratio of the observed nucleus ($s^{-1}.T^{-1}$)

g: gradient strength ($T.m^{-1}$)

The diffusion coefficient is then the slope of the line obtained by plotting $\ln(I/I_0)$ against $q^2.\left(\Delta - \frac{\delta}{3} - \frac{\tau}{2}\right)$

Spherical hydrodynamic radius

The spherical hydrodynamic radius (called Stokes radius) of the molecule was calculated from the Stokes-Einstein equation and compared to the value obtained from the solid state structure and with a similar reference compound in the same solvent:

$$r_{sph}\ (r_{sph} = \frac{k_B.T}{6\pi.\eta.D})$$

η ($Pa.s^{-1}$) = viscosity of the medium, k_B ($m^2.kg.s^{-2}.K^{-1}$) = Boltzmann constant.

T: absolute temperature (K), D: diffusion coefficient (m^2.s-1)

Results:

Table S5. Diffusion coefficient values of **1** and **2** and estimated spherical radii.

Solvent	Compound	D [m².s^{-1}]	r_{sph} [Å]$_{exp}$	r_{sph} [Å] (evaluated from crystal structure)
Pyridine η=0.879 mPa.s (298K)	**1**	3.29(4) 10^{-10}	7.5	8.5
	2	5.74(7) 10^{-10}	4.3	4.6

(1) Avens, L. R.; Bott, S. G.; Clark, D. L.; Sattelberger, A. P.; Watkin, J. G.; Zwick, B. D. *Inorg.Chem.* 1994, **33**, 2248-2256.
(2) Enriquez, A. E.; Scott, B. L.; Neu, M. P. *Inorg. Chem.* 2005, **44**, 7403-7413.
(3) Natrajan, L.; Burdet, F.; Pecaut, J.; Mazzanti, M. *J. Am. Chem. Soc.* 2006, **128**, 7152-7153.
(4) Shuppert, J. W.; Angell, C. A. *J.Chem. Phys.* 1977, **67**, 3050-3056.
(5) Brown, I. D.; Altermatt, D.; *Acta Cryst. B* 1985, **B41**, 244-247.
(6) Brown, I. D. http://www.ccp14.ac.uk/ccp/web-mirrors/i_d_brown/bond_valence_param/, 2009, and references therein.
(7) Tanner, J. E. *J. Chem. Phys.* 1970, **52**, 2523-2526.
(8) Wu, D. H.; Chen, A. D.; Johnson, C. S. *J. Magn. Reson. A* 1995, **115**, 260-264.
(9) Johnson, C. S. *Prog. Nucl. Magn. Reson. Spectrosc.* 1999, **34**, 203-256.